ACADEMIA ROMÂNĂ
Revue Roumaine de Chimie
http://web.icf.ro/rrch/

Rev. Roum. Chim.,
2017, *62*(12), 915-922

PERFORMANCES OF HYBRID SILICA-RHODAMINE B COMPOSITE PARTICLES IN Cu^{+2} DETECTION

Ligia TODAN,[a]* Mariana VOICESCU,[a] Daniela C. CULITA,[a] Cristina STAN[a] and Virgil MARINESCU[b]

[a] "Ilie Murgulescu" Institute of Physical Chemistry, Roumanian Academy, 202 Splaiul Independenței, 060021 Bucharest, Roumania
[b] National Institute for Research and Development in Electrical Engineering ICPE-CA, 313 Splaiul Unirii, 030138 Bucharest, Ruomania

Received November 3, 2016

Silica derived composite microparticles entrapping rhodamine B were synthesized through sol-gel process using different alkoxide precursors such as tetraethoxysilane (TEOS) and combinations of TEOS with its methyl and phenyl derivatives. Infrared spectroscopy, thermal analysis (DTG), nitrogen adsorption/ desorption measurements and scanning electron microscopy coupled with energy dispersive X-ray spectroscopy (SEM-EDS) have been used to characterize the phase evolution, pore structure, morphology and composition of the obtained powders. Their sensing abilities for Cu^{+2} in methanol were comparatively tested through fluorescence measurements. An interaction between the dye in the composite microparticles and Cu^{+2} was evidenced which depends on the structure of the host matrices and which generates photophysical changes in the colour and fluorescence emission intensity. In the presence of Cu^{+2}, methyl and phenyl substitution of TEOS matrix generate a more pronounced fluorescence quenching and a different but visible change of colour takes place in all samples.

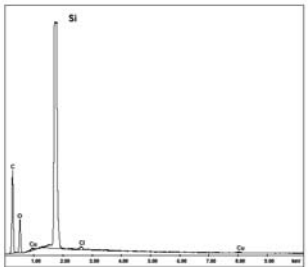

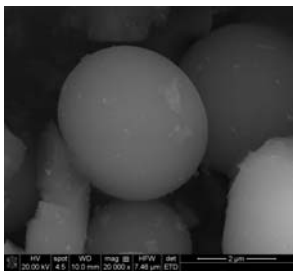

INTRODUCTION

The development of new colorimetric and fluorescent chemo sensors for the detection of the metal cations which are important for the environment and biological processes, has become very popular. Copper is one of the most studied elements due to its environmental and physiological role.[1, 2]

There is a high interest in the development of probes that are able to detect metal ions by fluorescence or colorimetric change due to the simplicity, quickness, low detection limit associated with optical techniques.[3]

Xanthene derivatives have interesting spectroscopic properties such as long absorption and emission wavelengths, large absorption coefficient, high fluorescence quantum yield that makes them ideal for constructing chemosensors.[4] Rhodamine dyes are often reported as reactive probes due to the fact that they have structure dependent spectral properties. This unique structural feature is that the spirocyclic form is nonfluorescent and colorless, whereas the ring-opened amide form is colored and fluorescent, process utilized for the detection of metal ions.[4,5]

The temperature dependence of the fluorescence spectrum of rhodamine B in $CuCl_2$ dyed glycerol was determined and it was found that Cu^{+2} enhances the infrared absorption coefficient of the sample for the wavelength of a 1064 nm pump laser.[6] Xanthene framework represents an ideal model to construct colorimetric and fluorescent chemosensors for Cu^{+2} and new derivatives with better detection properties were designed, synthesized and utilized in water

* Corresponding author: Dr. Ligia Todan (l_todan@yahoo.co.uk), Phone number: +40213167912; fax: +40213121147

systems.[1,2] Limitation of photostability, water insolubility, etc of organic dyes can be overcome by entrapping them inside a matrix and the obtained solid-state sensor materials have some advantages in terms of practicability.[7] For instance by encapsulating the dyes in a silica derived matrix, fluorescent sensing particles for technological and biomedical applications can be obtained.[7] ORMOSILs are versatile materials widely used for the development of sensors and in recent years different materials based on silica hybrids doped with colorants have been developed for optical detection.[8]

Silica nanoparticles embedding fluorescent dyes such as rhodamine B, with potential biotechnological applications have been synthesized and characterized.[9] Scarce details are given about fluoroionophore encapsulated in hybrid silica materials and their use as fluorescent particles in the detection of copper ions.

This study intends to be an investigation about the conditions to obtain by sol-gel method microparticles which consist of hybrid silica materials (tetraethylorthosilicate and combinations with its methyl and phenyl derivatives) as host matrices for rhodamine B (Rh B) as a model dye. Their optical performances in the presence of copper were determined, in correlation with their structure and composition. The non-hydrolysable organic groups bound to the silicon modify the properties of the host matrix and consequently the results will show how the xanthene dye interacts with organically modified silicas (ormosils) in the presence of Cu^{+2} and which will be the influence on its photophysical properties.

EXPERIMENTAL

Materials

Tetraethylorthosilicate (TEOS, Sigma-Aldrich), methyltriethoxysilane (MeTEOS, Fluka), phenyltriethoxysilane (PhTEOS, Merck), ethanol (Riedel-de Haën) were purchased from commercial suppliers. $CuCl_2$ was provided by Zoupin Runzi Chemical Industry.

Equipment

To get information about the stability and structure of the embedding matrices, thermo analyses of the powders without Rh B were conducted on a Metler Toledo 851e equipment in oxygen, with a heating rate of 10 ^oC/min, in the room-temperature-1000 ^oC range.

The specific surface area and pore characterization of the samples were determined by nitrogen adsorption at -196 ºC on a Micromeritics ASAP 2020 automated gas sorption system. The samples were outgased at 120 ºC for 3 hours under vacuum prior to N_2 adsorption. Specific surface areas (S_{BET}) were calculated according to Brunauer-Emmett-Teller (BET) equation using adsorption data in the relative pressure range 0.05 and 0.30 while pore size distributions were derived from the desorption branch using the Barrett–Joyner–Halenda (BJH) model. The total pore volume (V_{total}) was estimated from the amount adsorbed at the relative pressure of 0.99.

The variation of the structure of the Rh B containing powders, as prepared and in the presence of Cu^{+2} was determined by recording their infrared spectra on a Jasco FTIR 4100 instrument within the 4000-400 cm^{-1} range using KBr pellets.

The morphology of the samples was investigated by scanning electron microscopy (SEM) using a high-resolution microscope, FEI Quanta 3D FEG model, at an accelerating of 5 kV, in high vacuum. The images were recorded in secondary electron mode. The instrument is equipped with energy dispersive X-ray spectroscopy (EDS) for the elemental analysis.

The fluorescence spectroscopy evidenced changes of the optical properties of the microparticles in the presence of copper ions which are function of the silica matrix structure.

The fluorescence emission spectra of Rh B powders were recorded with a Jasco FP-6500 Spectrofluorometer, using 3 nm bandpasses for the excitation and the emission monochromators, the detector response of 1 sec, the scan rate of 100 nm/min, data pitch of 1 nm. The excitation wavelength was 510 nm.

Synthesis of composite particles

The precursor solutions were prepared by adding the following alkoxide combinations in ethanol: TEOS, TEOS-MeTEOS (1:1 molar ratio) and TEOS- PhTEOS (1:1 molar ratio).

The molar ratio Σprecursors/ ethanol was 1/6. The solutions were stirred in a 50 mL glass container. From a 10^{-4} molar solution of Rh B in methanol, 0.5 mL were added to each precursor solutions.

In the first acid hydrolysis step, an aqueous HCl solution was used to obtain a pH ≈ 2 of the mixture. After two hours of stirring at room temperature, in the second basic hydrolysis step, the pH was raised at ≈ 10 by adding an aqueous NH_4OH solution. The molar ratio Σprecursors/H_2O was 1/6.

Gelation time varied according to the solution composition: the first sample gelled instantly, the second one after 24 hours and the third one 30 days later. The samples were air-dried for 120 days and mixed from time to time so the final products were obtained as powders.

A stock solution of $CuCl_2$ in methanol 0.16 molar was prepared. Approximately 0.5 g of the powders were kept in about 30 cm^3 $CuCl_2$ solution for 30 min, separated and dried at 80^0C for an hour before the fluorescence measurements. The as prepared samples were pink and after being in contact with copper solution, a visual color response was generated (changes from intense pink to green-white in case of the TEOS derivative and to light pink in case of the TEOS-MeTEOS and TEOS-PhTEOS samples, a lighter shade for the Me derivative).

RESULTS AND DISCUSSION

Characterization of the silica matrices by thermal analysis

The thermal analysis of the powder matrices without Rh B was performed in order to determine the thermal stability and to better understand their structure.

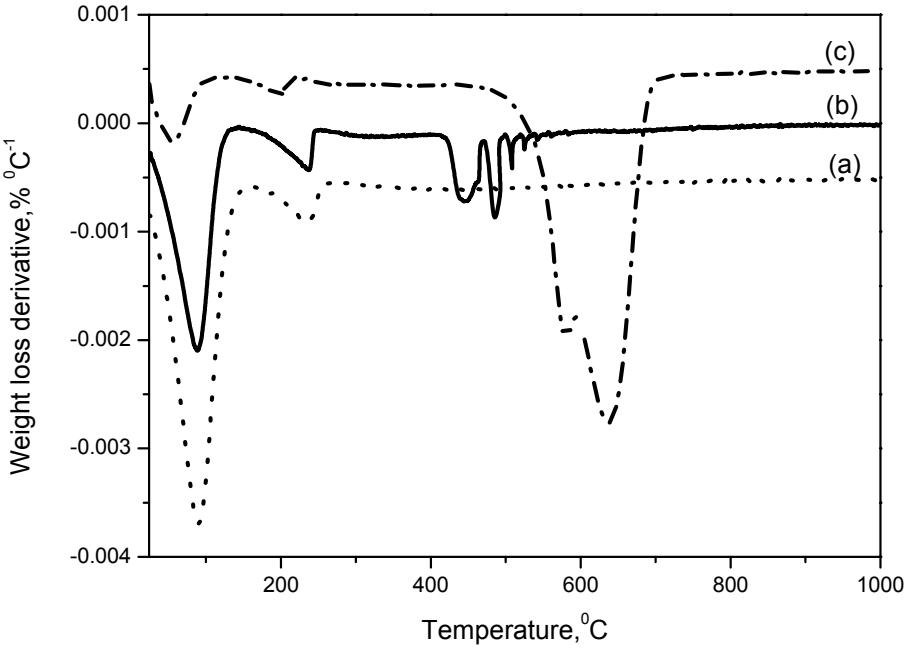

Fig. 1 – DTG thermograms of the powders without Rh B, in air: a) TEOS; b) TEOS- MeTEOS-; c) TEOS- PhTEOS.

Fig. 1 shows the DTG (first derivative) thermograms of TEOS, TEOS-MeTEOS and TEOS-PhTEOS gel matrices. In the first step up to 200°C, the mass loss in all three cases was attributed to the removal of physico-sorbed molecules, in particular water and ethanol.[10, 11] Since the surface silanol groups act as adsorption centres with greater affinity for water and polar solvents, the decrease of the mass loss in this stage, in the following order TEOS > TEOS- MeTEOS > TEOS- PhTEOS could be linked to the increase of the hydrophobic character with alkyl and phenyl substitution.[11]

The second step ranged from 200°C to 400°C in case of TEOS and TEOS- MeTEOS matrices, and 500°C in case of Ph substituted network respectively. The small mass variation in this step can be determined by the loss of water caused by the condensation of surface silanols.[10]

The third step was observed at temperatures greater than 400°C in case of TEOS and TEOS-MeTEOS matrices, and 500°C respectively in case of Ph substituted matrix. This step could be interpreted as a completion of the condensation reactions and the oxidation of organic groups (ethyl, methyl and phenyl).[10-12] The TEOS-MeTEOS DTG thermogram shows more peaks which correspond to the oxidation of the organic groups from different network fragments generated by the polymerization breaking due to the introduction of non-polymerizable methyl groups in the silica network.[13] The TEOS-PhTEOS matrix shows an important mass loss in this step corresponding to the oxidation of phenyl groups to CO_2 and H_2O.[10] The splitting of the peak on the DTG curve reveals a separation of two thermal events due to the existence of separate domains of the phenyl groups with different combustion properties.[10, 11, 14]

Determination of BET surface area and porosity

To gain insight into the porosity of the samples induced by the organosilane used in synthesis, we determined the surface area and pore volume of the samples by N_2 sorption analysis. As it is well known the nature and size of the network modifying agent plays a decisive role on material porosity and consequently on the specific surface area. The corresponding N_2 sorption isotherms together with the pore size distribution (PSD) graphs are shown in Fig. 2. The sample prepared using only TEOS as silica source and rhodamine B presented a type IV isotherm according to IUPAC classification, with H_2 hysteresis loop, characteristic for mesoporous materials. The BET specific surface area and pore volume were calculated as 488 $m^2\ g^{-1}$ and 0.392 $cm^3\ g^{-1}$ respectively. The PSD graph (inset of Fig. 2a) indicated a monomodal and relatively narrow pore size distribution with a BJH desorption average pore diameter of 3.1 nm. The introduction of

MeTEOS into the composition of the silica precursor resulted in a change of the isotherm shape comparing with the previous one, accompanied by a significant increase of S_{BET} value (798 $m^2 g^{-1}$). The total pore volume remained almost unchanged (0.445 $cm^3 g^{-1}$). The isotherm of TEOS-MeTEOS-Rh B sample was identified as a combination of type I and IV, indicating the presence of both micropores and mesopores in material.[10, 14] A careful examination of the isotherm revealed a small hysteresis in the range of relative pressure between 0.4 and 0.6, confirming the presence of mesopores in this sample. This observation was also confirmed by the PSD graph in which a small peak centered at 3 nm can be seen. The TEOS-PhTEOS-Rh B sample proved to be non-porous (isotherm not shown), the phenyl groups generating more dense and hydrophobic samples[14], in accordance with the thermal analysis results and due to more slowly curing of the gel, are preferentially localized on the exposed surfaces of pores and microchannels in the resulting siliceous material[15]. The textural characteristics of the samples determined by N_2 sorption analysis are in very good agreement with those obtained by SEM.

For comparative purposes the porosity of the silica matrices prepared without rhodamine B was also investigated. The sorption isotherms and PSD graphs of the silica matrices are similar to the corresponding ones of the samples with rhodamine (Fig. 2b), but the nitrogen adsorption capacity and the specific surface area slightly higher (Table 1). The silica matrix derived from TEOS- PhTEOS has been considered as non-porous since the adsorption volume was very small, 0.006 $cm^3 g^{-1}$ at $p/p_0 = 0.99$ (isotherm not shown).

The slight pore volume variation of the samples with and without Rh B suggests that the dye is mostly included inside the matrices and is not impregnated in the pores.

The dye comes into contact with the analyte not only due to the porosity of the matrix but also due to the swelling of the particles suggesting a gel-like internal structure.[15]

Evolution of the structure of the silica-Rh B prepared samples in the presence of Cu^{+2} studied by infrared spectroscopy

The infrared spectra of the composite rhodamine B-silica derived powders, displayed in figure 3 (a, b, c), show their evolution in the presence of Cu^{+2}. The samples exhibited typical Si-O-Si bands associated with the formation of a silica network in all three cases, present at about 1000-1300 cm^{-1}, 970 cm^{-1} and 800 cm^{-1}. [16, 17]

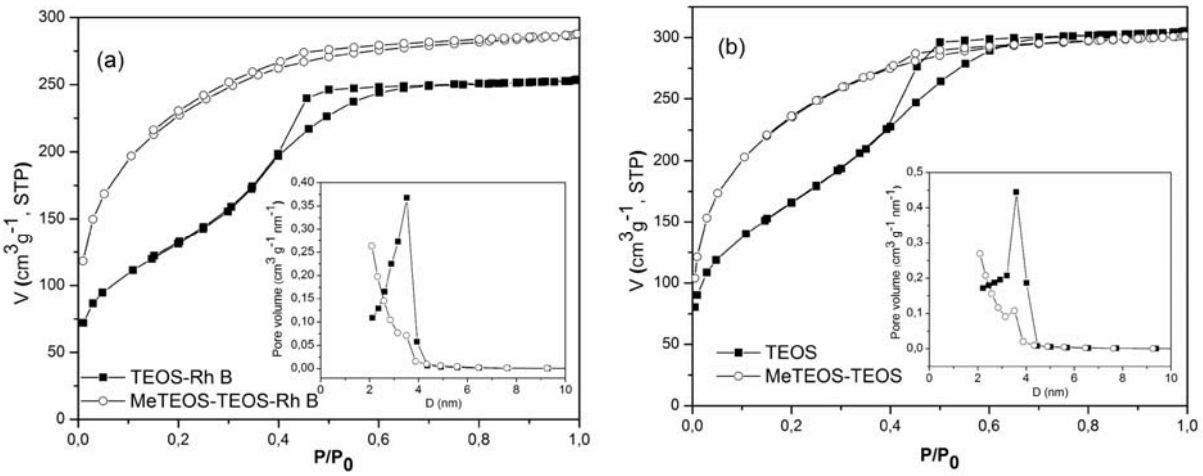

Fig. 2 – N_2 adsorption-desorption isotherms of (a) TEOS-RhB, MeTEOS-TEOS-RhB; (b) TEOS, MeTEOS-TEOS (inset – the corresponding PSD graphs).

Table 1

Specific surface area and pore volume of the matrices with and without Rh B

Sample	S_{BET} ($m^2 g^{-1}$)	V_{total} ($cm^3 g^{-1}$)
TEOS-Rh B	488	0.392
TEOS- MeTEOS-Rh B	798	0.445
TEOS matrix	606	0.472
TEOS- MeTEOS matrix	830	0.466

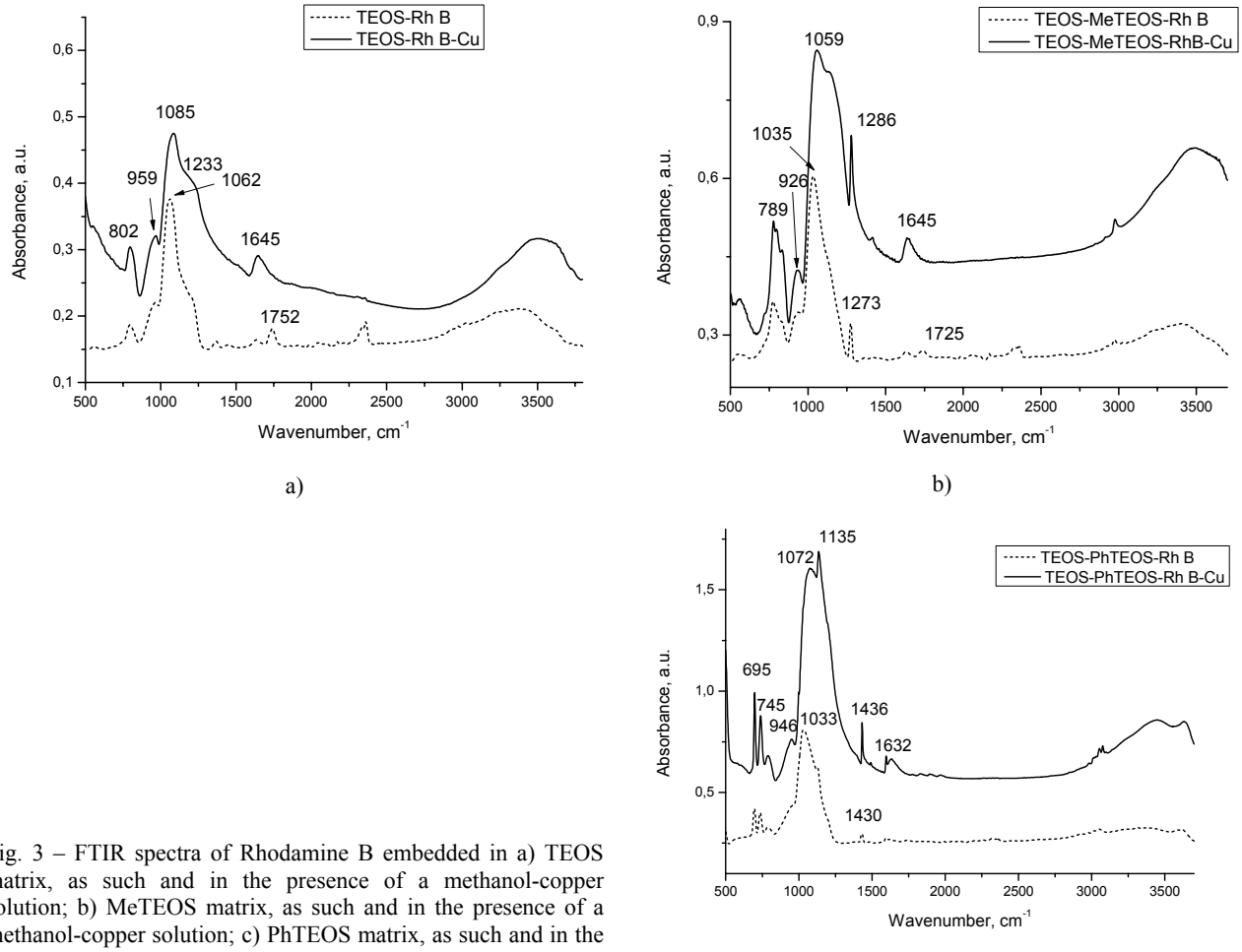

Fig. 3 – FTIR spectra of Rhodamine B embedded in a) TEOS matrix, as such and in the presence of a methanol-copper solution; b) MeTEOS matrix, as such and in the presence of a methanol-copper solution; c) PhTEOS matrix, as such and in the presence of a methanol-copper solution.

The organic substitution of the network shifts the ~1100 cm^{-1} ν (Si-O-Si) band to lower wavelengths. In the presence of Cu^{+2}, in case of each sample, a shift of this band to higher wavenumbers can be noticed indicating an interaction between the metal and the silica lattice.

In rhodamine IR spectrum two sets of vibrations can be distinguished, carboxylate and amino. C=O streching vibration is clearly shaped only in case of TEOS matrix at about 1720 cm^{-1} (fig. 2 a), it is very weak in the spectrum of the methyl derivative and disapears in case of the Ph substituted sample, confirming that the dye adsorbed on the silica matrix through the carboxyl group. [18] After immersion in $CuCl_2$-methanol solution the ν(C=O) band disapears and is replaced by the band at 1640-1630 cm^{-1} in the spectra of all three samples that could be associated to the antisymmetric streching vibration mode, ν_{as}(-COO), meaning that coordination to the metal may take place. [18, 19]

The bands characteristic for the amino group appear only in the spectra of the samples in contact with copper at about 1200-1100 cm^{-1}, slightly shifted from the values given in literature. [20] They can be seen as a shoulder in case of TEOS and MeTEOS sample and become a sharp peak for the phenyl derivative indicating the involvement of amino group in coordination with the metal. [20] The broad bands in the range 3000-3400 cm^{-1} can be assigned to the O-H and N-H streching vibrations of the hydrogen bonded groups. [19]

Characteristic peaks for methyl group develop at 1273 cm^{-1} and 789 cm^{-1} in the MeTEOS sample spectrum while in case of the phenyl substituted matrix peaks characteristic for ring streching and C-H bending appear at about 1430 cm^{-1} and respectively 700 cm^{-1}. [17]

The coordination of Rh B with Cu^{+2} as well as the interaction with the silica matrix can generate changes in the colour and fluorescence emission intensity due to the interruption of π-conjugation of the chromophore.[21]

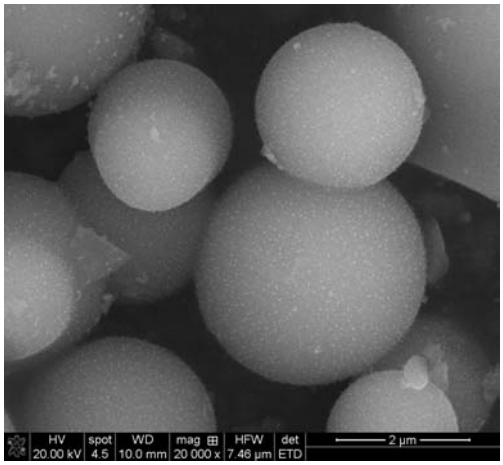

Fig. 4 – Micrograph of the composite TEOS-PhTEOS-Rh B-Cu powder.

Table 2

Elemental analysis of the particles from EDS results

Element	TEOS-RhB-Cu composite, At %	TEOS-MeTEOS-RhB-Cu composite, At %	TEOS-PhTEOS-RhB-Cu composite, At %
C K	19.98	35.80	64.86
N K	1.23	1.31	1.1
O K	27.10	21.06	11.44
Si K	52.01	41.27	23.22
Cl K	0.38	0.21	0.21
Cu K	0.40	0.35	0.28

Micro-structural and compositional details (SEM and EDS)

The morphology of the samples surface was investigated by SEM analysis, as can be seen in the micrograph in fig. 4. The TEOS and Me substituted TEOS powders exhibited particle agglomerates of irregular morphology but the TEOS-PhTEOS sample displayed large regular spherical micro agglomerates (fig. 4).

Energy dispersive X-ray spectroscopy (EDS) was performed to find out the composition of the silica matrices after the immersion in the copper solution (table 2).

From the table 2, one can see that beside the silica lattice represented by high silicon atomic percents, the presence of rhodamine can be guessed due to nitrogen values which are almost constant in the three samples. Copper was also included in the powders by physical and chemical bonds.

Fluorescence measurements in the presence of Cu^{2+}

Fig. 5 (a) shows the fluorescence emission spectra of TEOS/Me and Ph substituted matrix-Rh B systems. There is a decrease of Rh B fluorescence intensity in the organically substituted samples, more pronounced in case of Ph substituent which also generates a shift to higher wavelengths. In the presence of Cu^{+2}, a change of the fluorescence intensity as well as of the fluorescence emissions of Rh B in the matrices takes place. Comparing with the matrix without copper, the fluoresecence intensity strongly decreases, more significantly in the case of Me and Ph-substituted TEOS matrices, while the fluorescence emission is blue- or red- shifted as a function of matrix structure, Me and Ph-substituted network respectively (fig. 5, b). Comparing with the fluorescence emission spectrum of TEOS-Rh B sample, it can be observed that the fluorescence emission of TEOS matrix-Rh B in the presence of Cu^{2+} is ~20 nm hypsochromic shifted, λ_{em}= 555 nm. The feature is attributed to the coordination mode for Rh B with Cu^{2+} into the TEOS matrix. In direct comparison with TEOS matrix- Rh B-Cu, for Me-substituted TEOS matrix-Rh B-Cu, the fluorescence emission of Rh B appears at λ_{em}= 567 nm while in the case of Ph-substituted TEOS matrix-Rh B-Cu, the fluorescence emission of Rh B is 15 nm batochormic shifted, λ_{em} = 578 nm.

Also, the fluorescence intensity is strongly quenched. In this case, beside the coordination mode for Rh B with Cu^{2+}, the hydrozone forme of Rh B is considered. Fig. 5 (c) presents the corresponding fluorescence excitation spectra of TEOS/Me and Ph substituted TEOS matrix-Rh B-Cu systems. As can be seen, changes in the electronic absorption spectra of Rh B take place, the spectral range 375 - 450 nm, according to the influence of Me and Ph substituents of the TEOS based matrix.

Overall, the fluorescence of Rh B into the TEOS, Me/Ph-substituted TEOS matrix–Cu^{+2} is strongly quenched.

Beside fluorescence quenching which is more pronounced in methyl and phenyl derivatives, Cu^{+2} also generates a colorimetric response (visual color changes from intense shades of pink to green-white in case of the TEOS derivative, and light pink in case of the TEOS-MeTEOS and TEOS-PhTEOS samples, a lighter shade for the Me derivative). These effects can be due to interactions fluorophore-metal ion- matrix which breaks the configuration of the initial conjugated system of the dye and determines a different behavior of rhodamine B than the one mentioned in literature for the free fluorophore in a polyol.[22,23]

As well as in case of copper, Hg(II) excess is important for living organisms and for its detection optical sensing has also been applied using silica matrices with a rhodamine derivative.[23]

CONCLUSIONS

Silica based particles as a functional matrix for immobilizing fluorescent rhodamine B probe have been prepared by a sol-gel method from TEOS and its methyl and phenyl derivatives. The obtained matrices have satisfactory properties such as a stable structure up to 400^0C and a large ratio of surface to volume.

Interactions dye-silica matrix-copper were evidenced, generating changes in the colour and fluorescence emission intensity which depend on the structure of the host matrices.

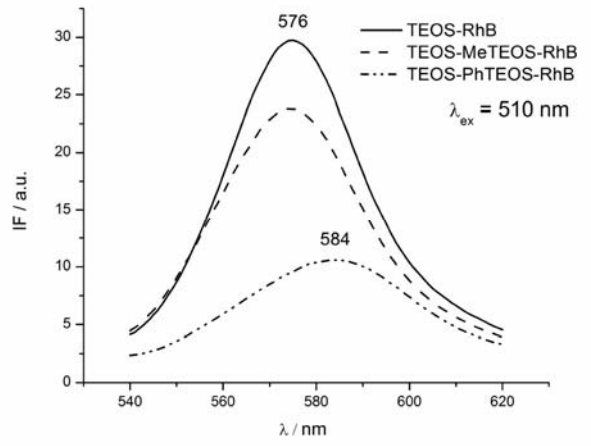

a)

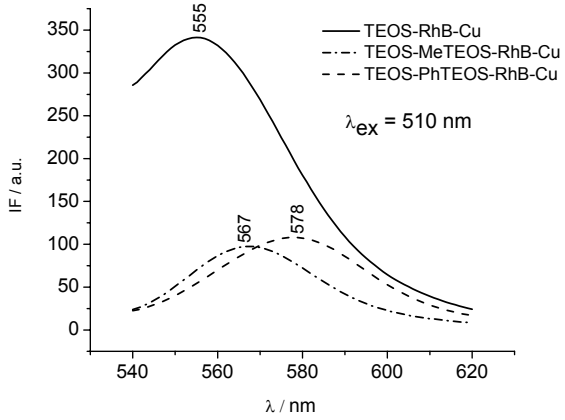

b)

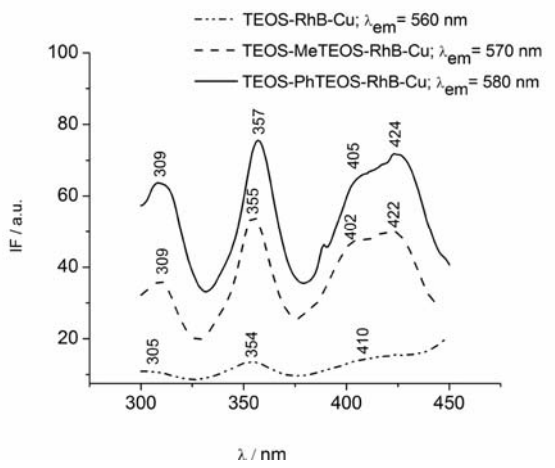

c)

Fig. 5 – Fluorescence emission spectra of TEOS/Me and Ph substituted matrix-RhB systems in the absence of Cu^{+2} (a); fluorescence emission spectra of the same Rh B matrices in the presence of Cu^{+2} (b); excitation spectra in the presence of Cu^{+2} (c).

The linking of the dye with the silica network prevented its leakage.

Upon the presence of the metal, Rh B molecule in all three matrices coordinates with generating a non-emissive structure. As a result, the fluorescence of the microparticles is strongly quenched, more significantly in the case of Me and Ph-substituted TEOS matrices and a 'turn-off' signal is perceived.

A color change accompanies the structural transformations providing another sensing channel of colorimetry.

REFERENCES

1. S. K. Kempahanumakkagaari and R.T. P. Malingappa, *J. Lumin.*, **2014,** *146*, 11-17.
2. Z. Xua, L. Zhang, R. Guo, T. Xiang, C. Wu, Z. Zheng and F. Yang, *Sens.Actuators*, B, **2011**, *156***,** 546-552.
3. S.M.S. Pires, C. Núñez, V.V. Serra, A. Sánchez-Coronilla, M.A.F. Faustino, M.M.Q.Sim□es, A.M.S. Silva, M.G.P.M.S. Neves, J.L.Capelo and C. Lodeiro, *Dyes and Pigments,* **2016**, *135*, 113-126.
4. J. Hu, Z, Hu, Y. Cui, X. Zhang, H.-W. Gao and K. Uvdal, *Sens.Actuators*, B, **2014**, *203*, 452-458.
5. Y. Hu, J. Zhang, Y.-Z. Lv, H.-H. Huang and S.-l. Hu, *Spectrochim. Acta Mol. Biomol. Spectrosc.*, **2016**, *157*, 164-169.
6. L. Liu, S. Creten, Y. Firdaus, J. J. A. F. Cuautle, M. Kouyaté, M. Van der Auweraer and C. Glorieu, *Appl. Phys. Lett.,* **2014**, *104*, 031902-1-031902-5.
7. A.S. Al Dwayan, S.M.H. Qaid, M.A.M. Khan and M.S. Al Salhi, *Opt. Mater.*, **2012**, *34***,** 761-768.
8. A. Raditoiu, V. Raditoiu, D.C. Culita, A. Baran, D. F. Anghel, C.I. Spataru, V. Amariutei, C. A. Nicolae, and L.E. Wagner, *Opt. Mater*., **2015**, *45,* 55-63.
9. E.C.C. Gomes, I.M.M. De Carvalho, I.C.N. Diógenes, E.H.S. De Sousa and E. Longhinotti, *Opt. Mater.,* **2014**, *36***,** 1197-1202.
10. P. Moriones, X. Ríos, J.C. Echeverría, J.J. Garrido, J. Pires and M. Pinto, *Colloids Surf. A Physicochem. Eng. Asp*., **2011**, *389,* 69-75.
11. X. Ríos, P. Moriones, J.C. Echeverría, A. Luquin, M. Laguna and J.J. Garrido, *Adsoption*, **2011**, *17***,** 583-593.
12. M. Nocuń, R. Gajerski and S. Siwulski, *Opt. Appl*., **2005**, *XXXV***,** 901-906.
13. X. Ríos, P. Moriones, J.C. Echeverría, A. Luquin, M. Laguna and J.J. Garrido, *Mater. Chem*. *Phys.,* **2013**, *141***,** 166-174.
14. S. Ulke and H. Koller, *Solid State Nucl. Magn. Reson*., **2011**, *39***,** 142-150.
15. S. Dash, S.Mishra, S. Patel and B.K. Mishra, *Adv. Colloid Interface Sci*., 2008, **140,** 77-94.
16. L. Todan, C. Andronescu, D. M. Vuluga, D. C. Culita and M. Zaharescu, *J.Therm. Anal*. *Calorym.*, **2013,** *114***,** 91-99.
17. B. Schyrr, S. Pasche, E. Scolan, R. Ischer, D. Ferrario, J-A. Porchet and G.Voirin, *Sens.Actuators, B,* 2014, *194***,** 238-248.
18. M.A. Jhonsi, A. Kathiravan and R. Renganathan, *J.Mol. Struct.,* **2009,** *921,* 279-284.
19. M. Tabatabaee, M. Bordbar, M. Ghassemzadeh, M. Tahriri, M. Tahrir, Z. M. Lighvan and B. Neumůller, *Eur. J.Med. Chem*., **2013,** *70***,** 364-371.
20. M. Avram and Gh. D. Mateescu, "Spectroscopia în infraroşu, Aplicaţii în Chimia Organică", Editura Tehnica Bucureşti, Roumania, 1966, p. 378-383.
21. M. Beija, C.A.M. Afonso and J.M.G. Martinho, *Chem. Soc. Rev*., **2009**, *38***,** 2410-2433.
22. S. Suganya, S. Velmathi and D. MubarakAli, *Dyes Pigments*, **2014**, *104*, 116-122.
23. Y. Chen and S. Mu, *J Lumin*, **2014**, *145*, 760-766.